crystals

MDPI

Review

Challenges and Opportunities for the Blue Perovskite Quantum Dot Light-Emitting Diodes

Shuchen Weng [1], Guicheng Yu [1], Chao Zhou [1,2], Fang Lin [1], Yonglei Han [1,2], Hao Wang [1], Xiaoxi Huang [1], Xiaoyuan Liu [1], Hanlin Hu [1], Wei Liu [3], Yongfei Wang [3] and Haoran Lin [1,*]

[1] Hoffman Institute of Advanced Materials, Shenzhen Polytechnic, 7098 Liuxian Blvd., Shenzhen 518000, China; totemroshu@szpt.edu.cn (S.W.); shenxia@szpt.edu.cn (G.Y.); czhou2205@163.com (C.Z.); linfang0318@szpt.edu.cn (F.L.); hyl19990130@163.com (Y.H.); wanghao@szpt.edu.cn (H.W.); xiaoxihuang@szpt.edu.cn (X.H.); liuxiaoyuan1989@szpt.edu.cn (X.L.); hanlinhu@szpt.edu.cn (H.H.)

[2] School of Materials and Metallurgy, University of Science and Technology Liaoning, 185 Qianshan Zhong Road, Anshan 114051, China

[3] School of Chemical Engineering and Technology, Sun Yat-Sen University, Zhuhai 519000, China; liuwei96@mail.sysu.edu.cn (W.L.); wyf8307@ustl.edu.cn (Y.W.)

* Correspondence: hlin@szpt.edu.cn

Abstract: Perovskite quantum dots (PQDs), as the promising materials for the blue light-emitting diodes (LEDs), own huge advantages as ultra-high color purity, flexibility and whole-spectrum tunability. Through dimensional and compositional engineering, PQD-LEDs have shown superiority in deep-blue light emission. However, compared with the fast development of red and green PeLEDs, the electroluminescent performance of PQD-LEDs has faced more obstacles. In this review, we aim to explore and state the uniqueness and the possible solutions for the bottleneck problems of the PQD-LEDs.

Keywords: perovskite quantum dots; blue-light emission; light-emitting diodes; dimensional engineering; compositional engineering

Citation: Weng, S.; Yu, G.; Zhou, C.; Lin, F.; Han, Y.; Wang, H.; Huang, X.; Liu, X.; Hu, H.; Liu, W.; et al. Challenges and Opportunities for the Blue Perovskite Quantum Dot Light-Emitting Diodes. *Crystals* **2022**, *12*, 929. https://doi.org/10.3390/cryst12070929

Academic Editors: M. Ajmal Khan and Dmitry Medvedev

Received: 21 May 2022
Accepted: 27 June 2022
Published: 30 June 2022

1. Introduction

When talking about the state-of-art perovskite light-emitting diodes (PeLEDs), perovskite quantum dots (PQDs) will never be neglected. Perovskite-related nanocrystals (NCs) with quantum-confinement effect are generally considered as quantum dots in this short review on the research frontier of blue perovskite quantum-dot LEDs (PQD-LEDs).

The developing tendency of the electroluminescence devices provides a hint to the design of light-emitting perovskites, namely, the wide color gamut, flexibility [1], stability and high color purity. Compared with the maturely commercialized organic LEDs (OLEDs), PQD-LEDs are outstanding for their ultra-high color purity, high luminance and much shorter response time. Additionally, the easy production with solution process and cost effectiveness add a bonus. The high-quality display requires precise segmentation of the color map by pixels. Since the first room-temperature PeLED appeared in public view, the device luminance, external quantum efficiency (EQE) and stability of the red and green PeLEDs began to thrive rapidly and may approach the dawn of practical application. However, the blue PeLEDs emitting the remaining one of the three primary colors are still in their infancy, which is roughly presented in Figure 1 and Table 1. Unlike the red and green PeLEDs, the highest EQEs of blue PeLEDs still lie in the range of 10–15% without balanced luminance, the full width at half maxima (FWHM) and device lifetime. From the conventional three-dimensional to the low-dimensional perovskites, from the bulk perovskites to perovskite nanocrystals, piles of experiments using different strategies to achieve high-performance blue PeLEDs gradually clarify the reasons for this disparity, which will be demonstrated later.

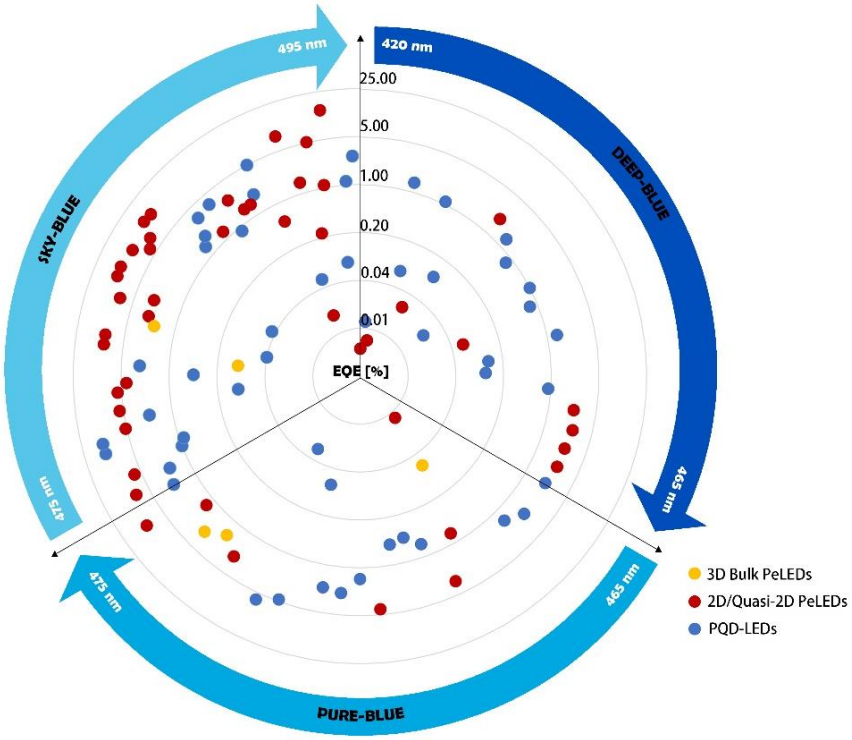

Figure 1. The distribution of EQE of some blue PeLEDs and PQD-LEDs. The division of sky-blue, pure-blue and deep-blue are based on the criteria by Rec. 2020 [1].

In this short review, other than enumerating the status quo of blue PQD-LEDs, we focus on the uniqueness of PQD-LEDs among the PeLEDs and the possible solutions for the bottle-neck problems of PQD-LEDs.

2. Basic

2.1. Blue Light-Emitting Perovskite Quantum Dot Materials

Despite the size-dependent quantum-confinement effect, PQDs share the same ABX_3 chemical formula as conventional metal halide perovskites, possessing a three-dimensional (3D) inorganic framework formed by corner-sharing $[BX_6]^{4-}$ octahedra. In the case of blue light-emitting PQDs, B-site is Pb^{2+} by default and X-site stands for Cl^- Br^-, or I^-. PQDs have several advantages over traditional 3D bulk perovskites regarding the light-emitting properties, which are the following: (1) PQDs exhibit enhanced radiative recombination over the nonradiative recombination, thus effectively improving the corresponding photoluminescence quantum yield (PLQY); (2) The maximum radiative recombination probability can be achieved by the highly spatially confined excitons; (3) The excitons in PQDs could generate strong symmetry-breaking perturbation, which further leads to light-activated forbidden exciton transition. All these characters can be attributed to the quantum confinement effect, resulting in outstanding potentials of PQDs in the blue light-emitting device [2].

2.2. The Basic Stack of PQD-LEDs

The device structures of PQD-LEDs are similar to that of other PeLEDs, including *n-i-p* or *p-i-n* architectures (Figure 2). In general, the fabrication of PQD-LEDs begins with the fabrication of electron-transport layers (*n-i-p* architectures) or hole-transport layers (*p-i-n* architectures) on the transparent electrode. Then, the PQD layers are deposited by methods including solution spin-coating or vacuum deposition, followed by the successful fabrication of the corresponding hole- or electron-transport layers and electrodes.

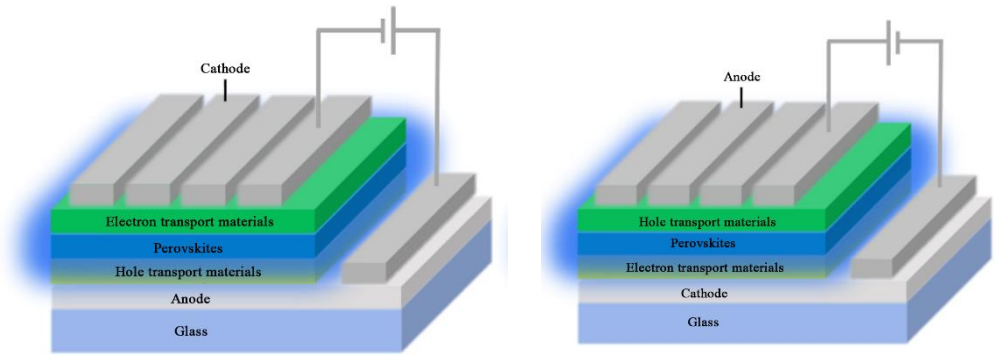

(**a**) (**b**)

Figure 2. (**a**) Typical *p-i-n* architecture of PeLED; (**b**) Typical *n-i-p* architecture of PeLED. Reprinted with permission from Ref. [1]. 2020, China Association for Science and Technology.

The commonly used electron transport materials and hole transport materials with their energy levels are summarized in Figure 3. The transporting layer materials include inorganic metal oxide materials with high stability and low cost and organic materials with the facile fabrication process and good conductivity [3–5]. The most commonly applied hole transport layer (HTL), poly(3,4-ethylenedioxythiophene):polystyrene sulfonate (PEDOT:PSS), has high conductivity, but suffers from hydrophilicity and luminescence quenching at the perovskite/PEDOT:PSS interface due to the charge energy transport barrier [6,7]. ZnO, as a commonly used inorganic electron transport layer (ETL) material, shows priority in water- and oxygen-resistance, assisting the fabrication of PQD-LEDs with relatively long lifetime [8,9]. To attain effective electroluminescence devices, the energy-level matching of the functional layers, the conductivity and stability of charge transport materials and the interfacial reactions should be carefully evaluated.

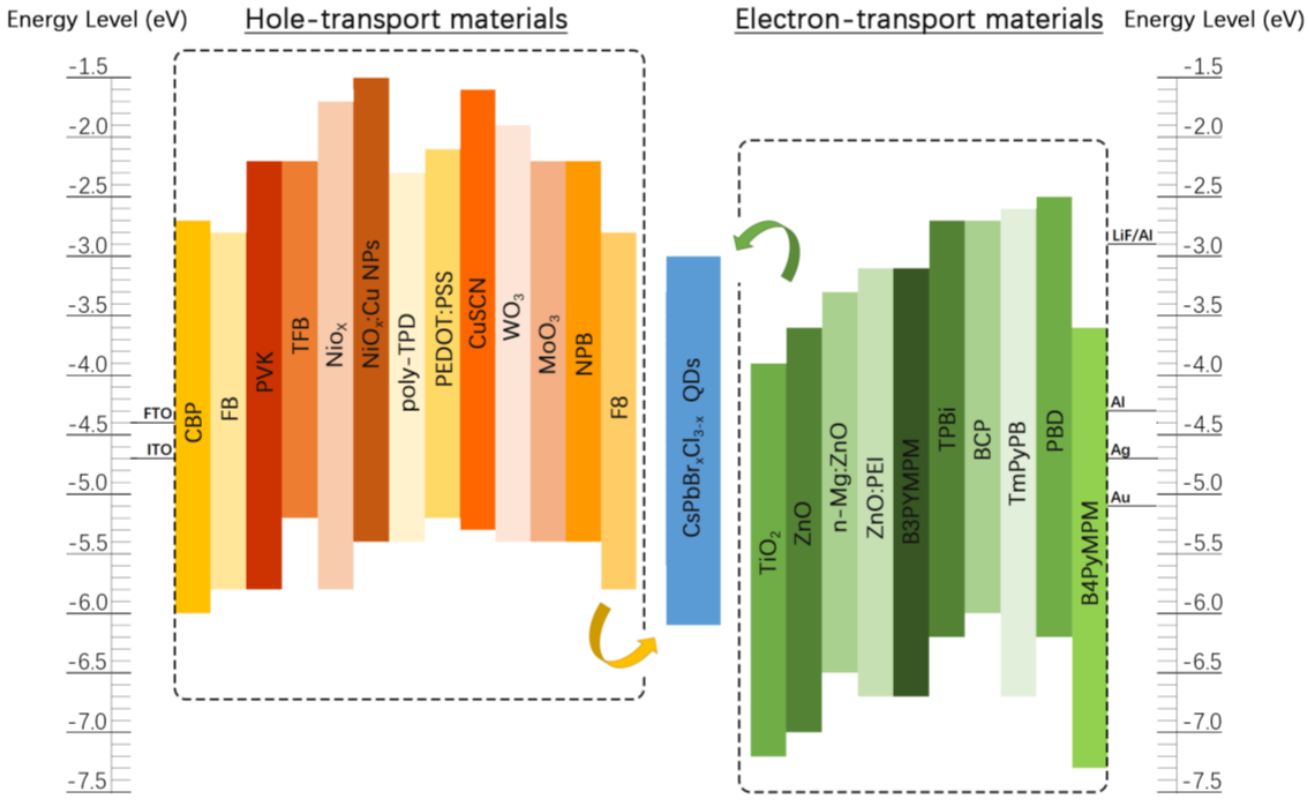

Figure 3. The energy diagram of the commonly used functional layers in PQD-LEDs.

Table 1. The overview of the performance of some blue PQD-LEDs in recent years.

Perovskites	Device Structure	EL Peak [nm]	$V_{turn-on}$ [V]	L_{max} [cd·m^{-2}]	EQE_{max} [%]	FWHM [nm]	LT_{50}	Year	Ref.
		Sky-blue PeLEDs							
$CsPbBr_xCl_{3-x}$	ITO/PEDOT:PSS/poly-TPD/perovskite/TPBi/Ca/Ag	496	3.2	603	2.6	18		2020	[10]
$CsPb(Br_{1-x}Cl_x)_3$	ITO/TiO_2/perovskite/F8/MoO_3/Au	495	4	750	0.075			2016	[11]
$CsPbBr_{2.4}Cl_{0.6}$	ITO/PEDOT:PSS/PVK/perovskite/TPBi/LiF/Al	495	7.8	2452	1.13	21		2016	[12]
$CsPbBr_xCl_{3-x}$	ITO/:ZnO/b-PEI/perovskite/PVK/V_2O_5/Al	492		143.1	0.053	26		2021	[13]
$CsPbBr_xCl_{3-x}$	ITO/PEDOT:PSS/polyTPD/PVK/perovskite/B3PYMPM/TPBi/LiF/Al	490	<3.4	2063	3.5	18–20	26 s@100 cd·m^{-2}	2019	[14]
$Rb_xCs_{1-x}PbBr_3$	ITO/PEDOT:PSS/poly-TPD/perovskite/TPBi/LiF/Al	490	4	186	0.87	22		2019	[15]
$CsPb(Br_{1-x}Cl_x)_3$	ITO/PEDOT:PSS/perovskite/TPBi/LiF/Al	490	3	35	1.9	19		2016	[16]
$(Cs/FA)PbBr_xCl_{3-x}$:Cu	ITO/PEDOT:PSS/PTAA/perovskite/TOPO/TPBi/LiF/Al	490	2.6	130	5.02	19		2020	[17]
$CsPbBr_xCl_{3-x}$	ITO/PEDOT:PSS/poly-TPD/perovskite/TPBi/Ca/Ag	489	3.4	182	1.8	18		2020	[10]
$CsPbBr_xCl_{4-x}$:La	ITO/PEDOT:PSS/PVK/perovskite/TPBi/LiF/Al	489	4	192.6	3.25	21		2020	[18]
$CsPbBr_xCl_{3-x}$	ITO/PEDOT:PSS/TFB/PFI/perovskite/TPBI/LiF/Al	488		830	1.41	23		2018	[19]
$CsPbBr_xCl_{3-x}$	ITO/ZnO/b-PEI/perovskite/PVK/V_2O_5/Al	486		94.2	0.045	25		2021	[13]
$CsPbBr_xCl_{3-x}$	ITO/ZnO/b-PEI/perovskite/PVK/V_2O_5/Al	484		95.1	0.04	25		2021	[13]
$CsPbBr_xCl_{3-x}$	ITO/PEDOT:PSS/TFB/PFI/perovskite/TPBI/LiF/Al	481		212	0.44	23		2018	[19]
$CsPbBr_xCl_{3-x}$:Nd	ITO/PEDOT:PSS/TFB/perovskite/TPBi/Liq/Al	481	3	138	2.7	14		2020	[20]
$CsPbBr_xCl_{3-x}$:La	ITO/PEDOT:PSS/PVK/perovskite/TPBi/LiF/Al	480	4	292.7	2.17	22		2020	[18]
$CsPbBr_3$ (nanoplates)	ITO/PEDOT:PSS/Poly-TPD/perovskite/TPBi/LiF/Al	480		25	0.1			2018	[21]
$CsPbBr_xCl_{3-x}$	ITO/PEDOT:PSS/poly-TPD/perovskite/TPBi/Ca/Ag	479	3.2	119	1	18		2020	[10]
$CsPbBr_xCl_{3-x}$	ITO/PEDOT:PSS/poly-TPD/perovskite/TPBi/LiF/Al	479	3.5	29.95	0.864	18		2019	[22]
$CsPbBr_3$	ITO/PEDOT:PSS/PTAA/perovskite/MoO_x/Ag	479		90	12.3	20	20 min@90 cd·m^{-2}	2020	[23]
$(K/Cs)PbBr_xCl_{3-x}$	ITO/PEDOT:PSS/poly-TPD/perovskite/TPBi/LiF/Al	477	3.2	86.95	1.96	19		2020	[24]
$CsPbBr_xCl_{3-x}$	ITO/PEDOT:PSS/polyTPD/PVK/perovskite/B3PYMPM/TPBi/LiF/Al	476	<3.4	678	2.25	18–20	26 s@100 cd·m^{-2}	2019	[14]
		Pure-blue PeLEDs							
$CsPbBr_xCl_{3-x}$	ITO/ZnO/b-PEI/perovskite/PVK/V_2O_5/Al	472		46.6	0.027	25		2021	[13]
$CsPb(Br_xCl_{1-x})_3$	ITO/TFB/PFI/MHP perovskite/3TPYMB/Liq/Al/Pt	471		465	6.3	17		2020	[25]
$CsPbBr_xCl_{3-x}$:Mn	ITO/TFB/PFI/perovskite/TPBi/LiF/Al	470	~4.8	389	1.46	17		2018	[26]
Ni^{2+}-$CsPbCl_xBr_{3-x}$	ITO/PEDOT:PSS/TFB/PFI/perovskite/TPBi/LiF/Al	470	3.2	612	2.4			2020	[27]
$CsPbCl_xBr_{3-x}$	ITO/PEDOT:PSS/polyTPD/PVK/perovskite/TmPyPB/TPBi/LiF/Al	470	4.9	507	2.15	21		2020	[28]
$CsPbCl_xBr_{3-x}$	ITO/NiOx/perovskite/TPBi/LiF/Al	470		350	0.07	20		2017	[29]
$CsPbBr_3$	ITO/PEDOT:PSS/PVK/perovskite/ZnO/Ag	470		3850	4.7	27	12 h@102 cd·m^{-2}	2021	[30]
$CsPbBr_xCl_{3-x}$	ITO/PEDOT:PSS/poly-TPD/perovskite/TPBi/Ca/Ag	469	3.8	30	0.65	18		2020	[10]
$CsPbBr_xCl_{3-x}$	ITO/PEDOT:PSS/poly-TPD/perovskite/TPBi/LiF/Al	469	4	11.95	0.44	18		2019	[22]
$CsPbBr_xCl_{3-x}$	ITO/PEDOT:PSS/TFB:PFI/perovskite/TPBi/LiF/Al	469		111	0.5	24		2018	[19]
$CsPbBr_xCl_{3-x}$	ITO/PEDOT:PSS/polyTPD/PVK/perovskite/TmPyPB/TPBi/LiF/Al	468	4.8	620	1.53	20		2020	[28]
$(Rb/Cs)PbBr_xCl_{3-x}$:Ni	ITO/PEDOT:PSS/poly-TPD/perovskite/TPBi/LiF/Al	467	3.5	10.4	2.14	16		2020	[31]
$CsMn_yPb_{1-y}Br_xCl_{3-x}$	ITO/TFB/PFI/perovskite/TPBi/LiF/Al	466		245	2.12	18		2018	[26]

Table 1. *Cont.*

Perovskites	Device Structure	EL Peak [nm]	$V_{turn-on}$ [V]	L_{max} [cd·m^{-2}]	EQE_{max} [%]	FWHM [nm]	LT_{50}	Year	Ref.
		Deep-blue PeLEDs							
$CsPbBr_xCl_{3-x}$	ITO/PEDOT:PSS/polyTPD/PVK/perovskite/TmPyPB/TPBi/LiF/Al	465	4.6	518	0.92	19		2020	[28]
$Rb_xCs_{1-x}PbBr_3$	ITO/PEDOT:PSS/poly-TPD/perovskite/TPBi/LiF/Al	464	4	63	0.11	18		2019	[15]
$CsPb(Br/Cl)_3$	ITO/PEDOT:PSS/Poly-TPD/CBP/perovskite/B3PYMPM/LiF/Al	463	2.9	318	1.4	14		2019	[32]
$CsPbBr_3$	ITO/PEDOT:PSS/Poly-TPD/perovskite/TPBi/LiF/Al	463		62	0.124	12		2018	[33]
$CsPbBr_xCl_{3-x}$	ITO/ZnO/b-PEI/perovskite/PVK/V_2O_5/Al	462	5	32.5	0.02	24		2021	[13]
$CsPbBr_xCl_{3-x}$	ITO/PEDOT:PSS/polyTPD/PVK/perovskite/B3PYMPM/TPBi/LiF/Al	462	<3.4	193	1	18–20	26 s@100 cd·m^{-2}	2019	[14]
$CsPbBr_xCl_{3-x}$	ITO/PEDOT:PSS/polyTPD/PVK/perovskite/TmPyPB/TPBi/LiF/Al	462	4.4	450	0.77	19		2020	[28]
$CsPbBr_xCl_{3-x}$	ITO/PEDOT:PSS/poly-TPD/perovskite/TPBi/LiF/Al	461	4	763	0.8	16		2019	[34]
$CsPbCl_xBr_{3-x}$	ITO/PEDOT:PSS/Poly-TPD/perovskite/TPBi/LiF/Al	460	3.8	33	1.35	15	51.5 s@3.7 V	2019	[35]
$CsPbBr_xCl_{3-x}$	ITO/PEDOT:PSS/poly-TPD/perovskite/TPBi/LiF/Al	458	4.5	3.865	0.101	17		2019	[22]
$CsPb(Cl/Br)_3$	ITO/PEDOT:PSS/TFB/perovskite/TPBi/Liq/Al	456	5.4	43.2	1.1	16	5 s@10 cd·m^{-2}	2020	[36]
$CsPb(Cl/Br)_3$	ITO/PEDOT:PSS/PVK/perovskite/TPBi/LiF/Al	455	5.1	742	0.07	20		2015	[37]
$CsPbBr_{1.5}Cl_{1.5}$	ITO/PEDOT:PSS/PVK/perovskite/TPBi/LiF/Al	445	7.8	2673	1.38	<30		2016	[12]
$CsPbBr_xCl_{3-x}$	ITO/ZnO/b-PEI/perovskite/PVK/V_2O_5/Al	435	5	12.3	0.01	25		2021	[13]

3. Uniqueness of Blue PQDs and PQD-LEDs

3.1. High-Quality Blue Light Emission

3.1.1. LIGHT Tuning Strategies

As Table 2 depicts, there are two main paths to achieving the blue light emission of perovskite materials, which are compositional engineering and dimensional engineering (quantum-confinement engineering) of conventional bulk perovskite.

Table 2. Two strategies to achieve blue light-emitting perovskites and comparison in several aspects.

Performance	2D/Quasi-2D Perovskites	PQDs	3D Bulk Perovskites
Defects	Relatively passivated	More surface defects	Surface and bulk defects
FWHM	Relatively large	Small	Relatively large
PL performance	Good	Good	Poor
EL performance	Good	Poor	Poor
Stability	High	Moderate	Low

Compositional engineering tunes the A-, B- or X- sites individually or simultaneously for perovskites with the ABX_3 formula. Replacing the bromide with broader-bandgap chloride will efficiently enlarge the bandgap and thus blue-shifting the emission spectrum. However, all-chloride perovskites are rare to find in blue PeLEDs due to their naturally poor PLQY and stability. For mixed halide perovskites, manipulating the ratio of halides in ABX_3 can effectively tune the bandgap in the blue-light regions. However, the negative impacts brought by chloride are inevitable as well, such as the phase separation and ion migration under applied voltage, especially for the deep-blue PeLED devices. Another method of compositional engineering includes cation doping in A- or B-sites, individually or simultaneously. The doping-tuning is achieved by twisting the perovskite crystal structure and changing the metal–halide bond strengths/angles. More specifically, a broader bandgap is achieved by the decreased orbital overlap in a more distorted crystal lattice [38]. The major problem comes from the size discrepancy with the cation substitution, rewriting the tolerance factor of perovskites, and may lead to stability issues.

Dimensional engineering includes the structural-dimensional modification to develop two-dimensional/quasi-two-dimensional (2D/quasi-2D) perovskites with multiple-quantum-well structures and the morphological-dimensional modification to develop perovskite nanocrystals including quantum dots, which are nano-sized crystals keeping the same crystallographic feature with 3D perovskites. In general, the dimensional modified perovskites own better optical properties compared with 3D bulk perovskites due to their efficient radiative recombination and unique charge or energy transfer process [1]. Emission color tuning is achieved either by size control for perovskite nanocrystals or layer number control for quasi-2D perovskites. Other factors such as defects, surface ligands, morphology, and so on, also contribute to their spectral behavior.

PQDs could combine and balance the merits of both dimensional and compositional engineering to achieve best-performance PQD-LEDs. For example, Pan et al. [27] doped 2.5% Ni^{2+} into the $CsPbBr_xCl_{3-x}$ and sophisticated set the x at 2.01, attaining a high PLQY (89%) at 470 nm emission. The blue LED based on the modified PQDs exhibits an EQE of 2.4% and a max luminance of 612 $cd \cdot m^{-2}$.

3.1.2. Deep-Blue Emission

As Figure 1 demonstrates, among the rapidly developing blue PeLEDs, the EQEs of the deep-blue and pure-blue devices are lagging behind that of the sky-blue devices. To achieve highly efficient deep-blue and pure-blue LEDs for display applications, the strategy using PQD materials is most likely to succeed based on the following analysis. For 3D bulk PeLEDs: (1) Deep-blue emission requires a large bandgap and high ratio of chloride content, leading to deep trap states and poor EL performance; (2) Under high applied bias and high carrier density (Figure 4), the increased ion-migration and phase

separation brings instability to the system. For 2D/quasi-2D PeLEDs: (1) Large bandgap requires a low-n structure (n means the inorganic layer number for quasi-2D perovskites $B_2A_{n-1}Pb_nX_{3n+1}$ [39]), which requires an elaborate film fabrication process to obtain a narrow distribution of n; (2) Due to the energy funneling effect, the emission of the quasi-2D PeLEDs represents the emission of quasi-2D composition with the highest n value, which set obstacles to achieving deep-blue emission.

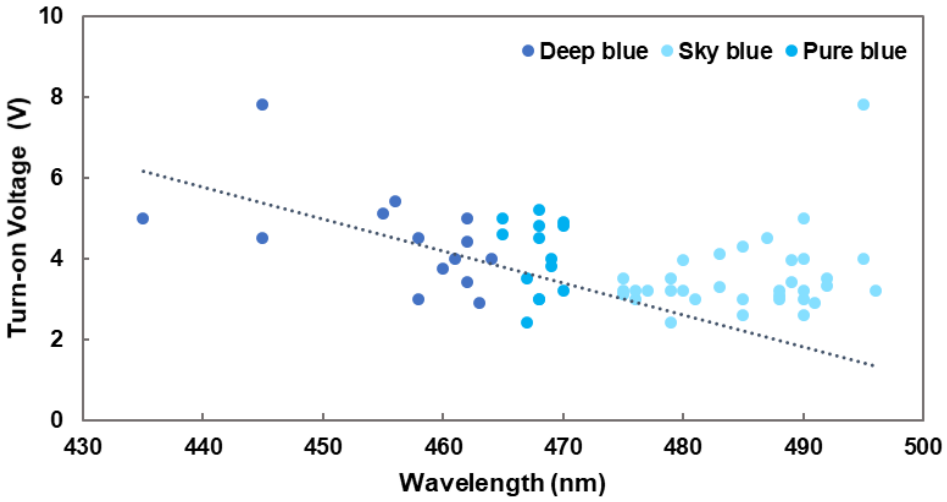

Figure 4. The trend of turn-on voltage along with their emission wavelengths for some representative PeLEDs.

On the other hand, PQDs hold gorgeous potential in the blue and deep-blue region since their emission can be tuned through the size-dependent quantum confinement effect, which escapes the thread brought by the mixed halide. The size and morphology of the PQDs can be precisely manipulated using proper synthetic methods. For instance, Dong et al. [40] developed a unique size-controlling method from the aspect of thermodynamic equilibrium in the synthesis process and achieved $CsPbX_3$ QDs with high size-uniformity. Meanwhile, Parobek et al. [41] reported another direct hot-injection synthesis method for Mn^{2+} doped $CsPbBr_3$ NCs and demonstrated the relationship between the addition of HBr and the particle sizes. Yang et al. [42] applied a more complex method to precisely control the $CsPbCl_xBr_{3-x}$ ($0 < x \leq 3$) QDs by forming polymer gel networks with $CsPbBr_3$ precursors combined with the utilization of passivators. Additionally, the surrounding organic chain can efficiently alleviate the ion migration, and thus improve the stability under high applied bias. In the case, PQDs own a much greater stake in the application possibility.

3.2. Stability of PQD-LEDs

3.2.1. Material Stability

- Ambient stability

PQDs have intrinsic advantages in ambient stability owing to the protection of the surrounding organic ligands or the unique core/shell structures. Ge et al. [43] demonstrated that the 0D Cs_4PbX_6 can serve as a nice choice for encapsulating the $CsPbX_3$ QDs. This kind of encapsulation effectively prolongs the operation stability in the ambient environment [44] meanwhile increases the PLQY [45]. The ambient stability could also be improved through ion doping. For example, Zou et al. [46] reported a structurally unchanged outcome under a temperature as high as 200 °C by means of Mn^{2+} doping to $CsPbBr_3$ QDs. Conversely, if the protective layer of the PQDs is damaged for some reason, the PQDs could easily go through aggregation or degradation which is detrimental for PQD-LED devices.

- Spectral stability

Spectral shift is always induced by intrinsic factors, including phase separation, aggregation and degradation of PQDs, or by extrinsic factors such as heat, light, electric field, film morphology, etc. [47]. To solve the phase separation problem of the mix-halide PQD-LEDs, using all-bromide PQDs is proven to be an effective method to obtain better spectral stability. Additionally, interfacial engineering is considered to be another efficient way to mitigate defect-induced spectral instability. On the other hand, by optimizing the film quality and thickness, the extrinsic risks can be largely reduced. Heat or light stimulation could also induce aggregation by surface ligands desorption of the PQDs [30]. This problem can be solved by ligand modification to a large extent.

3.2.2. Device Stability

Device stability, quantified by the operation time for devices to retain half of the initial luminance (LT_{50}), received extension by defect passivation and ligand exchange as well. Ion migration, as stated above, appears within almost all kinds of perovskites and PeLEDs and induces overshoot of luminance over operation time. Due to the ionic nature of halogen-perovskites, this inherent drawback weighs more on the mixed-halide perovskites [48]. The bulky organic ligand on the surface of PQDs effectively blocks the ion migration channel, thus significantly improving the operational stability of the devices [49]. From Chen et al. [50], another lifetime limitation factor for blue PQD-LEDs should be attributed to the fast degradation at the QD-ETL junction. They emphasized that excited electrons in blue QDs are prone to accumulating in the QD-ETL junction and therefore induced an inner voltage rise in the ETL. The possible solution could be ETL engineering or introducing multiple layers for energy cascade. Therefore, it is necessary to further investigate the influence brought by the interfacial energy mismatch and possible electrochemical reaction on the PQD-LED devices. The design of chemical and electrochemical inert transport layer materials also plays a critical role in achieving PQD-LED devices with long-term stability [51,52].

3.3. Defect Passivation

As stated above, all bromide or mixed-halide PQDs are promising candidates for high-efficiency blue PQD-LEDs. However, the existing LED devices based on PQDs still have relatively poor performance compared with the state-of-art devices based on quasi-2D perovskites. One main reason is that the surface defect density of PQDs is extremely high due to the ultra-high surface-to-volume ratio. Another reason is that deep defect states are likely to form in the large bandgap of the blue emitters. Meanwhile, to achieve deep-blue emission, a small particle size of PQDs is needed, thus requiring a lower synthesis temperature accompanied by slower growth kinetics. As a result, not only a large surface-to-volume ratio is inevitable, but the fast crystal growth also generates additional defect sites on the PQDs. The defects in PQDs could serve as traps in the recombination process, which are detrimental to their luminescence performance [53]. The defect problem is one of the main obstacles for developing high-performance PQD-LEDs for practical application. Conversely, defect engineering enables valuable opportunities to further improve their photoluminescence and electroluminescence properties. In fact, some PQDs are reported to have near-unity PLQY after surface passivation as illustrated below.

The A site and B site vacancies can be passivated by ion doping. As Chiba et al. [20] summarized in their work, transition metals (including Mn^{2+}, Ni^{2+}, Cd^{2+}, Y^{3+}, etc.), alkaline metals (include Ca^{2+}, Sr^{2+}), Lanthanoids (include Ce^{3+} and Eu^{3+}) and some other bivalent or trivalent metal ions such as Sn^{2+}, Mg^{2+} and Bi^{3+} are capable of defect passivation. They found that the Nd^{3+} cation can effectively incorporate with $CsPbBr_xCl_{3-x}$ to suppress the nonradiative recombination, reaching a high PLQY of 97% and exhibiting a maximum EQE of 2.7% for the corresponding PQD-LED devices.

The ammonium functional group has strong interaction with lead halide octahedrons, which is capable of passivating the A-site vacancies. Lewis-base ligands with lone-pair electrons or additional halide anions in turn can interact with lead dangling bonds and

passivate the halogen vacancies [54]. Therefore, OAm (oleylamine) and OA (oleic acid) are commonly used in the synthesis of perovskite quantum dots. OA can prevent the agglomeration of PQDs and OAm controls the large grain formation [10]. However, these ligands bind weakly to the QD-surface and interchangeable dynamic equilibrium exists, resulting in the reagglomeration and more surface defects during device fabrication [30]. Different alkyl ammoniums and carboxylic acids were tested for their defect passivation ability. Other types of ligands such as phosphonic acids, zwitterions, or even polymers are also considered as stability-guarantee candidates due to their neutralization-resist ability [10] or strong binding ability with the PQD surface, which simultaneously improves the device performance and stability of PQD-LEDs [36]. In a representative case [30], HBr etching was first applied to remove the surface imperfect $[PbX_6]^{4-}$ octahedrons, then didodecylamine and phenethylamine were induced to provide a shorter-chain environment for charge injection. The resulting $CsPbBr_3$ QDs achieved a near-unity PLQY of 97% and a considerable EQE (4.7%) of the device. Additionally, a delightful operation lifetime (LT_{50} > 12 h@105 cd·m^{-2}) at 470 nm was attained.

3.4. The Balance between Photoluminescence and Electroluminescence

Some tags are always tightly linked with PQDs nearly since it was invented, typically high PLQY and poor EQE. The different mechanism between photoluminescence and electroluminescence of PQD-LEDs is responsible for this discrepancy. The participation of long-chain ligands such as commonly used OA/OAm is inevitable in the synthetic methods of PQDs. These long-chain ligands benefit room-temperature preservation and are sometimes helpful for their PLQY due to minimized interfacial energy loss. However, in contrast to the photoluminescence process triggered by direct excitation of photons, the electroluminescence process involves charge injection from outside the PQDs. The long-chain ligands usually possess poor conductivity resulting in a much higher internal resistance and Joule heat during operation, eventually leading to the high turn-on voltage and poor stability of PQD-LEDs, especially for the deep-blue devices. To solve this problem, short ligands or dilute-ligand structures are brought in to improve the preferable electrical properties of the PQDs [55]. As an illustration, ligands with benzene rings could enhance the charge transport between adjacent QDs through π-conjugation [30]. Pu et al. [55] modified their core/shell PQDs with the method of electrochemically-inert ligand replacement, sacrificing the PLQY from ~80% to ~60%, but significantly enhancing the peak EQE from lower than 4% to approximately 10%. The balance between the photoluminescence and electroluminescence properties of PQDs should be comprehensively taken into account to meet various application scenarios.

3.5. Superior Light Purity

Among the light-emitting parameters of LEDs, color purity determined by the FWHM of the emission peak is essential for high-quality display applications. The high color purity could be the most predominant advantage of PQD-LEDs over commercially available LEDs, where the FWHM for most PeLEDs is generally as small as ~20 nm (Table 1), much narrower than the commercial FWHM criteria. The core-shell structure together with the quantum-confinement effect bring in this outstanding feature [55]. For PQDs, the uniform size distribution, homogenous crystal structure and low trap density [30] are the key factors for narrow FWHM. Ultra-narrow FWHMs are witnessed for PQD-LEDs based on Nd^{3+} modified $CsPbBr_xCl_{3-x}$ with merely 14 nm at 481 nm [20], 14 nm at 463 nm for undoped $CsPbBr_xCl_{3-x}$ [32] and inspiring 12 nm at 463 nm for $CsPbBr_3$ [33], while most blue 2D/quasi-2D PeLEDs are with mediate-narrow FWHMs of around 25 nm.

4. Summary and Outlook

In conclusion, enhanced electroluminescence performance of PQD-LEDs can be achieved by ligand engineering, morphology control, transporting layers design, etc. [30] However, as shown in Table 3, the state-of-the-art PQD-LEDs still possess unsatisfactory

EQE and device lifetime, far from the stage of real applications [55]. The basic commercial requirements for displays should be at least several tens of thousands of hours [56]. Furthermore, the long-term spectral stability under high luminance also put forward a huge challenge for PQD-LEDs.

Table 3. Lifetime comparison of PeLEDs and OLEDs Reprinted with permission from Ref. [56]. 2021, Springer Nature.

	PeLEDs			**OLEDs**		
LT_{50} (hours)	Blue	Green	Red	Blue	Green	Red
	0.4	11	112	11,000	400,000	250,000

L_0 (initial luminance) = 1000 cd·m^{-2}.

Although industrialization seems too early for PQD-LEDs, we evaluate its rise in space and commercial value with unbounded optimism. As Woo et al. [56] mentioned in their work, compared with the 30 years of development of OLEDs before commercialization, PeLEDs needed less than 10 years to burst into a consideration-worthy level. Prompted by the increasing research intensity in this field, we believe the PQD-LED technology could eventually make breakthroughs and embrace its bright future.

Author Contributions: Writing—original draft preparation, S.W., G.Y. and C.Z.; data collection, F.L. and Y.H.; writing—review and editing, H.W., X.H., X.L., H.H., W.L. and Y.W.; supervision, H.L. All authors have read and agreed to the published version of the manuscript.

Funding: This research was funded by National Natural Science Foundation of China, grant number 201901166, 22005202. And the APC was funded by Scientific Research Startup Fund for Shenzhen High-Caliber Personnel of SZPT, grant number 6022310054k.

Institutional Review Board Statement: Not applicable.

Informed Consent Statement: Not applicable.

Data Availability Statement: Not applicable.

Conflicts of Interest: The authors declare no conflict of interest.

References

1. Zou, G.; Chen, Z.; Li, Z.; Yip, H.-L. Blue Perovskite Light-emitting Diodes: Opportunities and Challenges. *Acta Phys. Chim. Sin.* **2021**, *37*, 2009002. [CrossRef]
2. He, H.; Mei, S.; Wen, Z.; Yang, D.; Yang, B.; Zhang, W.; Xie, F.; Xing, G.; Guo, R. Recent Advances in Blue Perovskite Quantum Dots for Light-Emitting Diodes. *Small* **2022**, *18*, 2103527. [CrossRef] [PubMed]
3. Song, J.; Li, J.; Xu, L.; Li, J.; Zhang, F.; Han, B.; Shan, Q.; Zeng, H. Room-Temperature Triple-Ligand Surface Engineering Synergistically Boosts Ink Stability, Recombination Dynamics, and Charge Injection toward EQE-11.6% Perovskite QLEDs. *Adv. Mater.* **2018**, *30*, 1800764. [CrossRef]
4. Meng, L.; Yao, E.P.; Hong, Z.; Chen, H.; Sun, P.; Yang, Z.; Li, G.; Yang, Y. Pure Formamidinium-Based Perovskite Light-Emitting Diodes with High Efficiency and Low Driving Voltage. *Adv. Mater.* **2017**, *29*, 1603826. [CrossRef] [PubMed]
5. Wang, Z.; Yuan, F.; Sun, W.; Shi, H.; Hayat, T.; Alsaedi, A.; Fan, L.; Tan, Z.A. Multifunctional p-Type Carbon Quantum Dots: A Novel Hole Injection Layer for High-Performance Perovskite Light-Emitting Diodes with Significantly Enhanced Stability. *Adv. Opt. Mater.* **2019**, *7*, 1901299. [CrossRef]
6. Wang, Z.; Cheng, T.; Wang, F.; Dai, S.; Tan, Z. Morphology Engineering for High-Performance and Multicolored Perovskite Light-Emitting Diodes with Simple Device Structures. *Small* **2016**, *12*, 4412–4420. [CrossRef]
7. Yuan, M.; Quan, L.N.; Comin, R.; Walters, G.; Sabatini, R.; Voznyy, O.; Hoogland, S.; Zhao, Y.; Beauregard, E.M.; Kanjanaboos, P.; et al. Perovskite energy funnels for efficient light-emitting diodes. *Nat. Nanotechnol.* **2016**, *11*, 872–877. [CrossRef]
8. Liu, L.; Wang, Z.; Sun, W.; Zhang, J.; Hu, S.; Hayat, T.; Alsaedi, A.; Tan, Z. All-solution-processed perovskite light-emitting diodes with all metal oxide transport layers. *Chem. Commun.* **2018**, *54*, 13283–13286. [CrossRef]
9. Shi, Z.; Li, S.; Li, Y.; Ji, H.; Li, X.; Wu, D.; Xu, T.; Chen, Y.; Tian, Y.; Zhang, Y.; et al. Strategy of Solution-Processed All-Inorganic Heterostructure for Humidity/Temperature-Stable Perovskite Quantum Dot Light-Emitting Diodes. *ACS Nano* **2018**, *12*, 1462–1472. [CrossRef]
10. Ye, F.; Zhang, H.; Wang, P.; Cai, J.; Wang, L.; Liu, D.; Wang, T. Spectral Tuning of Efficient $CsPbBr_xCl_{3-x}$ Blue Light-Emitting Diodes via Halogen Exchange Triggered by Benzenesulfonates. *Chem. Mater.* **2020**, *32*, 3211–3218. [CrossRef]

11. Yassitepe, E.; Yang, Z.; Voznyy, O.; Kim, Y.; Walters, G.; Castañeda, J.A.; Kanjanaboos, P.; Yuan, M.; Gong, X.; Fan, F.; et al. Amine-Free Synthesis of Cesium Lead Halide Perovskite Quantum Dots for Efficient Light-Emitting Diodes. *Adv. Funct. Mater.* **2016**, *26*, 8757–8763. [CrossRef]
12. Deng, W.; Xu, X.; Zhang, X.; Zhang, Y.; Jin, X.; Wang, L.; Lee, S.-T.; Jie, J. Organometal Halide Perovskite Quantum Dot Light-Emitting Diodes. *Adv. Funct. Mater.* **2016**, *26*, 4797–4802. [CrossRef]
13. Park, Y.R.; Kim, H.H.; Eom, S.; Choi, W.K.; Choi, H.; Lee, B.R.; Kang, Y. Luminance efficiency roll-off mechanism in $CsPbBr_{3-x}Cl_x$ mixed-halide perovskite quantum dot blue light-emitting diodes. *J. Mater. Chem. C* **2021**, *9*, 3608–3619. [CrossRef]
14. Shynkarenko, Y.; Bodnarchuk, M.I.; Bernasconi, C.; Berezovska, Y.; Verteletskyi, V.; Ochsenbein, S.T.; Kovalenko, M.V. Direct Synthesis of Quaternary Alkylammonium-Capped Perovskite Nanocrystals for Efficient Blue and Green Light-Emitting Diodes. *ACS Energy Lett.* **2019**, *4*, 2703–2711. [CrossRef]
15. Todorović, P.; Ma, D.; Chen, B.; Quintero-Bermudez, R.; Saidaminov, M.I.; Dong, Y.; Lu, Z.H.; Sargent, E.H. Spectrally Tunable and Stable Electroluminescence Enabled by Rubidium Doping of $CsPbBr_3$ Nanocrystals. *Adv. Opt. Mater.* **2019**, *7*, 1901440. [CrossRef]
16. Pan, J.; Quan, L.N.; Zhao, Y.; Peng, W.; Murali, B.; Sarmah, S.P.; Yuan, M.; Sinatra, L.; Alyami, N.M.; Liu, J.; et al. Highly Efficient Perovskite-Quantum-Dot Light-Emitting Diodes by Surface Engineering. *Adv. Mater.* **2016**, *28*, 8718–8725. [CrossRef]
17. Chen, F.; Xu, L.; Li, Y.; Fang, T.; Wang, T.; Salerno, M.; Prato, M.; Song, J. Highly efficient sky-blue light-emitting diodes based on Cu-treated halide perovskite nanocrystals. *J. Mater. Chem. C* **2020**, *8*, 13445–13452. [CrossRef]
18. Zhang, S.; Liu, H.; Li, X.; Wang, S. Enhancing quantum yield of $CsPb(Br_xCl_{1-x})_3$ nanocrystals through lanthanum doping for efficient blue light-emitting diodes. *Nano Energy* **2020**, *77*, 105302. [CrossRef]
19. Gangishetty, M.K.; Hou, S.; Quan, Q.; Congreve, D.N. Reducing Architecture Limitations for Efficient Blue Perovskite Light-Emitting Diodes. *Adv. Mater.* **2018**, *30*, 1706226. [CrossRef]
20. Chiba, T.; Sato, J.; Ishikawa, S.; Takahashi, Y.; Ebe, H.; Sumikoshi, S.; Ohisa, S.; Kido, J. Neodymium Chloride-Doped Perovskite Nanocrystals for Efficient Blue Light-Emitting Devices. *ACS Appl. Mater. Interfaces* **2020**, *12*, 53891–53898. [CrossRef]
21. Yang, D.; Zou, Y.; Li, P.; Liu, Q.; Wu, L.; Hu, H.; Xu, Y.; Sun, B.; Zhang, Q.; Lee, S.-T. Large-scale synthesis of ultrathin cesium lead bromide perovskite nanoplates with precisely tunable dimensions and their application in blue light-emitting diodes. *Nano Energy* **2018**, *47*, 235–242. [CrossRef]
22. Shin, Y.S.; Yoon, Y.J.; Lee, K.T.; Jeong, J.; Park, S.Y.; Kim, G.H.; Kim, J.Y. Vivid and Fully Saturated Blue Light-Emitting Diodes Based on Ligand-Modified Halide Perovskite Nanocrystals. *ACS Appl. Mater. Interfaces* **2019**, *11*, 23401–23409. [CrossRef] [PubMed]
23. Dong, Y.; Wang, Y.K.; Yuan, F.; Johnston, A.; Liu, Y.; Ma, D.; Choi, M.J.; Chen, B.; Chekini, M.; Baek, S.W.; et al. Bipolar-shell resurfacing for blue LEDs based on strongly confined perovskite quantum dots. *Nat. Nanotechnol.* **2020**, *15*, 668–674. [CrossRef] [PubMed]
24. Yang, F.; Chen, H.; Zhang, R.; Liu, X.; Zhang, W.; Zhang, J.; Gao, F.; Wang, L. Efficient and Spectrally Stable Blue Perovskite Light-Emitting Diodes Based on Potassium Passivated Nanocrystals. *Adv. Funct. Mater.* **2020**, *30*, 1908760. [CrossRef]
25. Zheng, X.; Yuan, S.; Liu, J.; Yin, J.; Yuan, F.; Shen, W.-S.; Yao, K.; Wei, M.; Zhou, C.; Song, K.; et al. Chlorine Vacancy Passivation in Mixed Halide Perovskite Quantum Dots by Organic Pseudohalides Enables Efficient Rec. 2020 Blue Light-Emitting Diodes. *ACS Energy Lett.* **2020**, *5*, 793–798. [CrossRef]
26. Hou, S.; Gangishetty, M.K.; Quan, Q.; Congreve, D.N. Efficient Blue and White Perovskite Light-Emitting Diodes via Manganese Doping. *Joule* **2018**, *2*, 2421–2433. [CrossRef]
27. Pan, G.; Bai, X.; Xu, W.; Chen, X.; Zhai, Y.; Zhu, J.; Shao, H.; Ding, N.; Xu, L.; Dong, B.; et al. Bright Blue Light Emission of Ni^{2+} Ion-Doped $CsPbCl_xBr_{3-x}$ Perovskite Quantum Dots Enabling Efficient Light-Emitting Devices. *ACS Appl. Mater. Interfaces* **2020**, *12*, 14195–14202. [CrossRef]
28. Shao, H.; Zhai, Y.; Wu, X.; Xu, W.; Xu, L.; Dong, B.; Bai, X.; Cui, H.; Song, H. High brightness blue light-emitting diodes based on $CsPb(Cl/Br)_3$ perovskite QDs with phenethylammonium chloride passivation. *Nanoscale* **2020**, *12*, 11728–11734. [CrossRef]
29. Yao, E.P.; Yang, Z.; Meng, L.; Sun, P.; Dong, S.; Yang, Y.; Yang, Y. High-Brightness Blue and White LEDs based on Inorganic Perovskite Nanocrystals and their Composites. *Adv. Mater.* **2017**, *29*, 1606859. [CrossRef]
30. Bi, C.; Yao, Z.; Sun, X.; Wei, X.; Wang, J.; Tian, J. Perovskite Quantum Dots with Ultralow Trap Density by Acid Etching-Driven Ligand Exchange for High Luminance and Stable Pure-Blue Light-Emitting Diodes. *Adv. Mater.* **2021**, *33*, 2006722. [CrossRef]
31. Pan, J.; Zhao, Z.; Fang, F.; Wang, L.; Wang, G.; Liu, C.; Chen, J.; Xie, J.; Sun, J.; Wang, K.; et al. Multiple Cations Enhanced Defect Passivation of Blue Perovskite Quantum Dots Enabling Efficient Light-Emitting Diodes. *Adv. Opt. Mater.* **2020**, *8*, 2001494. [CrossRef]
32. Ochsenbein, S.T.; Krieg, F.; Shynkarenko, Y.; Raino, G.; Kovalenko, M.V. Engineering Color-Stable Blue Light-Emitting Diodes with Lead Halide Perovskite Nanocrystals. *ACS Appl. Mater. Interfaces* **2019**, *11*, 21655–21660. [CrossRef] [PubMed]
33. Wu, Y.; Wei, C.; Li, X.; Li, Y.; Qiu, S.; Shen, W.; Cai, B.; Sun, Z.; Yang, D.; Deng, Z.; et al. In Situ Passivation of $PbBr_6^{4-}$ Octahedra toward Blue Luminescent $CsPbBr_3$ Nanoplatelets with Near 100% Absolute Quantum Yield. *ACS Energy Lett.* **2018**, *3*, 2030–2037. [CrossRef]
34. Yang, D.; Li, X.; Wu, Y.; Wei, C.; Qin, Z.; Zhang, C.; Sun, Z.; Li, Y.; Wang, Y.; Zeng, H. Surface Halogen Compensation for Robust Performance Enhancements of $CsPbX_3$ Perovskite Quantum Dots. *Adv. Opt. Mater.* **2019**, *7*, 1900276. [CrossRef]

35. Zhang, B.B.; Yuan, S.; Ma, J.P.; Zhou, Y.; Hou, J.; Chen, X.; Zheng, W.; Shen, H.; Wang, X.C.; Sun, B.; et al. General Mild Reaction Creates Highly Luminescent Organic-Ligand-Lacking Halide Perovskite Nanocrystals for Efficient Light-Emitting Diodes. *J. Am. Chem. Soc.* **2019**, *141*, 15423–15432. [CrossRef] [PubMed]
36. Chiba, T.; Ishikawa, S.; Sato, J.; Takahashi, Y.; Ebe, H.; Ohisa, S.; Kido, J. Blue Perovskite Nanocrystal Light-Emitting Devices via the Ligand Exchange with Adamantane Diamine. *Adv. Opt. Mater.* **2020**, *8*, 2000289. [CrossRef]
37. Song, J.; Li, J.; Li, X.; Xu, L.; Dong, Y.; Zeng, H. Quantum Dot Light-Emitting Diodes Based on Inorganic Perovskite Cesium Lead Halides ($CsPbX_3$). *Adv. Mater.* **2015**, *27*, 7162–7167. [CrossRef]
38. Wang, H.; Zhao, X.; Zhang, B.; Xie, Z. Blue perovskite light-emitting diodes based on RbX-doped polycrystalline $CsPbBr_3$ perovskite films. *J. Mater. Chem. C* **2019**, *7*, 5596–5603. [CrossRef]
39. Jin, Y.; Wang, Z.K.; Yuan, S.; Wang, Q.; Qin, C.; Wang, K.L.; Dong, C.; Li, M.; Liu, Y.; Liao, L.S. Synergistic Effect of Dual Ligands on Stable Blue Quasi-2D
Perovskite Light-Emitting Diodes. *Adv. Funct. Mater.* **2019**, *30*, 1908339. [CrossRef]
40. Dong, Y.; Qiao, T.; Kim, D.; Parobek, D.; Rossi, D.; Son, D.H. Precise Control of Quantum Confinement in Cesium Lead Halide Perovskite Quantum Dots via Thermodynamic Equilibrium. *Nano Lett.* **2018**, *18*, 3716–3722. [CrossRef]
41. Parobek, D.; Dong, Y.; Qiao, T.; Son, D.H. Direct Hot-Injection Synthesis of Mn-Doped $CsPbBr_3$ Nanocrystals. *Chem. Mater.* **2018**, *30*, 2939–2944. [CrossRef]
42. Yang, H.; Feng, Y.; Tu, Z.; Su, K.; Fan, X.; Liu, B.; Shi, Z.; Zhang, Y.; Zhao, C.; Zhang, B. Blue emitting $CsPbBr_3$ perovskite quantum dot inks obtained from sustained release tablets. *Nano Res.* **2019**, *12*, 3129–3134. [CrossRef]
43. Ge, W.; Shi, J.; Tian, Y.; Xu, M.; Wu, Y.; Li, Y. Core-shell $CsPbBr_3$@Cs_4PbBr_6 nanocrystals dispersed in thermoplastic polyurethane as writeable heat-resistant fluorescent inks. *J. Alloy. Compd.* **2021**, *865*, 158768. [CrossRef]
44. Wang, Y.; Yu, D.; Wang, Z.; Li, X.; Chen, X.; Nalla, V.; Zeng, H.; Sun, H. Solution-Grown $CsPbBr_3/Cs_4PbBr_6$ Perovskite Nanocomposites: Toward Temperature-Insensitive Optical Gain. *Small* **2017**, *13*, 1701587. [CrossRef] [PubMed]
45. Quan, L.N.; Quintero-Bermudez, R.; Voznyy, O.; Walters, G.; Jain, A.; Fan, J.Z.; Zheng, X.; Yang, Z.; Sargent, E.H. Highly Emissive Green Perovskite Nanocrystals in a Solid State Crystalline Matrix. *Adv. Mater.* **2017**, *29*, 1605945. [CrossRef] [PubMed]
46. Zou, S.; Liu, Y.; Li, J.; Liu, C.; Feng, R.; Jiang, F.; Li, Y.; Song, J.; Zeng, H.; Hong, M.; et al. Stabilizing Cesium Lead Halide Perovskite Lattice through Mn(II) Substitution for Air-Stable Light-Emitting Diodes. *J. Am. Chem. Soc.* **2017**, *139*, 11443–11450. [CrossRef]
47. Bae, W.K.; Park, Y.S.; Lim, J.; Lee, D.; Padilha, L.A.; McDaniel, H.; Robel, I.; Lee, C.; Pietryga, J.M.; Klimov, V.I. Controlling the influence of Auger recombination on the performance of quantum-dot light-emitting diodes. *Nat. Commun.* **2013**, *4*, 2661. [CrossRef]
48. Dong, Q.; Lei, L.; Mendes, J.; So, F. Operational stability of perovskite light emitting diodes. *J. Phys. Mater.* **2020**, *3*, 012002. [CrossRef]
49. Kim, H.; Kim, J.S.; Heo, J.M.; Pei, M.; Park, I.H.; Liu, Z.; Yun, H.J.; Park, M.H.; Jeong, S.H.; Kim, Y.H.; et al. Proton-transfer-induced 3D/2D hybrid perovskites suppress ion migration and reduce luminance overshoot. *Nat. Commun.* **2020**, *11*, 3378. [CrossRef]
50. Chen, S.; Cao, W.; Liu, T.; Tsang, S.W.; Yang, Y.; Yan, X.; Qian, L. On the degradation mechanisms of quantum-dot light-emitting diodes. *Nat. Commun.* **2019**, *10*, 765. [CrossRef]
51. Wang, L.; Shi, Z.; Ma, Z.; Yang, D.; Zhang, F.; Ji, X.; Wang, M.; Chen, X.; Na, G.; Chen, S.; et al. Colloidal Synthesis of Ternary Copper Halide Nanocrystals for High-Efficiency Deep-Blue Light-Emitting Diodes with a Half-Lifetime above 100 h. *Nano Lett.* **2020**, *20*, 3568–3576. [CrossRef] [PubMed]
52. Jeong, J.E.; Park, J.H.; Jang, C.H.; Song, M.H.; Woo, H.Y. Multifunctional Charge Transporting Materials for Perovskite Light-Emitting Diodes. *Adv. Mater.* **2020**, *32*, 2002176. [CrossRef] [PubMed]
53. Nenon, D.P.; Pressler, K.; Kang, J.; Koscher, B.A.; Olshansky, J.H.; Osowiecki, W.T.; Koc, M.A.; Wang, L.W.; Alivisatos, A.P. Design Principles for Trap-Free $CsPbX_3$ Nanocrystals: Enumerating and Eliminating Surface Halide Vacancies with Softer Lewis Bases. *J. Am. Chem. Soc.* **2018**, *140*, 17760–17772. [CrossRef] [PubMed]
54. Noel, N.K.; Abate, A.; Stranks, S.D.; Parrott, E.S.; Burlakov, V.M.; Goriely, A.; Snaith, H.J. Enhanced Photoluminescence and Solar Cell Performance via Lewis Base Passivation of OrganicInorganic Lead Halide Perovskites. *ACS Nano* **2014**, *8*, 9815–9821. [CrossRef] [PubMed]
55. Pu, C.; Dai, X.; Shu, Y.; Zhu, M.; Deng, Y.; Jin, Y.; Peng, X. Electrochemically-stable ligands bridge the photoluminescence-electroluminescence gap of quantum dots. *Nat. Commun.* **2020**, *11*, 937. [CrossRef]
56. Woo, S.-J.; Kim, J.S.; Lee, T.-W. Characterization of stability and challenges to improve lifetime in perovskite LEDs. *Nat. Photonics* **2021**, *15*, 630–634. [CrossRef]